Journal Pre-proof

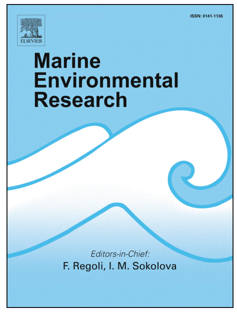

Phytoplankton dynamics based on satellite inherent optical properties and oceanographic conditions in a patagonian gulf frontal system in relation to the adjacent continental shelf waters

Rodrigo Hernández-Moresino, Gabriela N. Williams, Antonela Martelli, Elena S. Barbieri

PII: S0141-1136(21)00272-5

DOI: https://doi.org/10.1016/j.marenvres.2021.105516

Reference: MERE 105516

To appear in: *Marine Environmental Research*

Received Date: 4 May 2021

Revised Date: 28 September 2021

Accepted Date: 3 November 2021

Author statement

Rodrigo Hernández-Moresino and Gabriela Williams: conceptualization, methodology, formal analysis, investigation, writing - original draft. Antonela Martelli and Elena Barbieri: conceptualization, review, and editing.

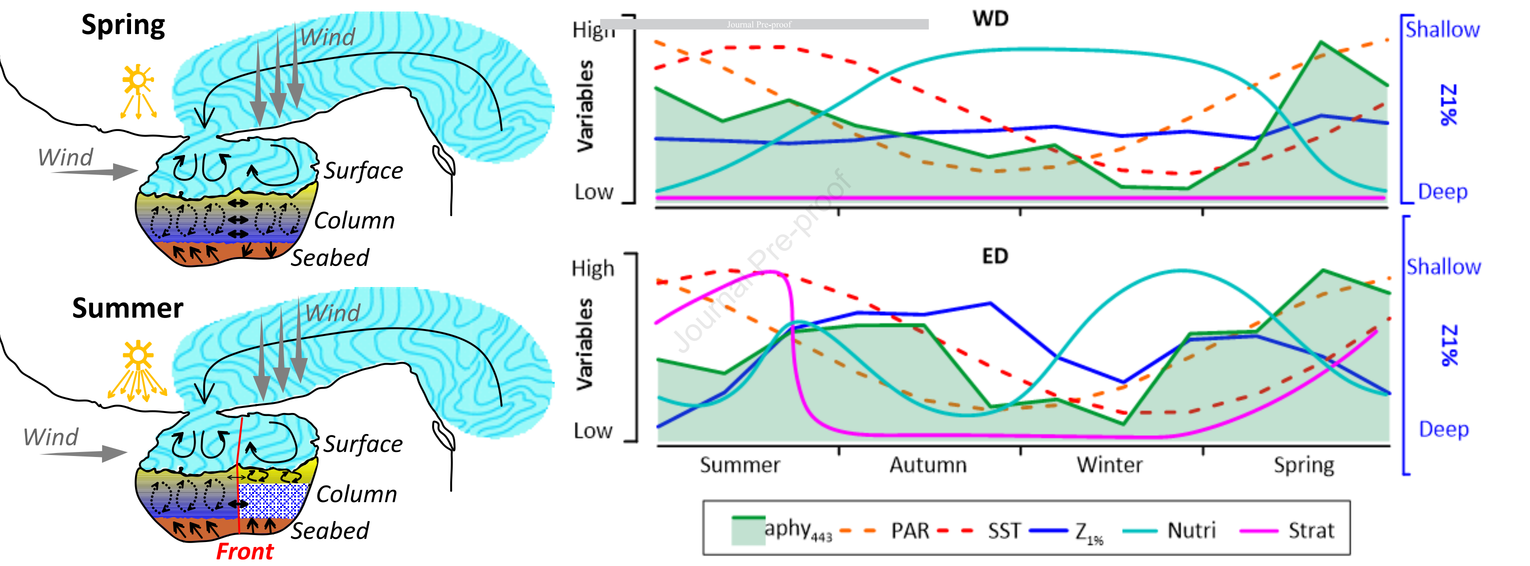
Spring
Wind
Wind
Surface
Column
Seabed
Summer
Wind
Wind
Surface
Column
Seabed
Front
WD
High
Low
Variables
Shallow
Z1%
Deep
ED
High
Low
Variables
Shallow
Z1%
Deep
Summer
Autumn
Winter
Spring
aphy443
PAR
SST
Z1%
Nutri
Strat

Phytoplankton dynamics based on satellite inherent optical properties and oceanographic conditions in a Patagonian gulf frontal system in relation to the adjacent continental shelf waters.

[1, 2]Rodrigo Hernández-Moresino, [1]Gabriela N. Williams*, [1, 2]Antonela Martelli,[1, 2]Elena S. Barbieri

[1]Centro para el Estudio de Sistemas Marinos (CESIMAR), Consejo Nacional de Investigaciones Científicas y Técnicas (CONICET), Edificio CCT CONICET – CENPAT.

[2]Instituto Patagónico del Mar (IPAM), Universidad Nacional de la Patagonia San Juan Bosco, sede Puerto Madryn.

*Corresponding author at Centro para el Estudio de Sistemas Marinos (CESIMAR - CCT CONICET-CENPAT), Bv. Almirante Brown 2915 (U9120ACD), Puerto Madryn, Chubut, Argentina. E-mail address: williams@cenpat-conicet.gob.ar

Abstract

The dynamics of phytoplankton across a seasonal frontal system formed in San José Gulf (SJG, Patagonia Argentina) and in neighbouring shelf waters was assessed based on bio-optical satellite data (2003-2018) and spring and summer *in situ* samplings. Bio-optical properties of the water masses on the eastern (ED) and western (WD) domains of the seasonal frontal system of SJG showed clear differences: the year-round-vertically-mixed waters from the WD, strongly connected with the adjacent shelf waters, evidenced a brief and strong single phytoplankton bloom, while those from the ED, showing lower exchange with shelf waters and a strong vertical stratification during the warm season, displayed an earlier and long-lasting spring phytoplankton bloom, followed by a late-summer and autumn bloom, both associated with the development and erosion of the seasonal thermocline. Waters from the entire system are optically influenced by the absorption of coloured dissolved organic matter and detritus (cdom + detritus), suggests a strong sediment load contribution from the continent and the seabed. To remark, a strong correlation between satellite chlorophyll-a (Chla-sat) and absorption by phytoplankton ($aphy_{443}$) in the outer shelf waters differs from the weak correlation of those variables in the gulf's water masses, whose optical parameters are more complex. *In situ* Chla records may indicate wind-driven upwelling and downwelling areas in the northern and southern coasts of the ED. Dissolved nitrogen was identified as the limiting macronutrient for phytoplankton growth in the ED during summer. This work contributes relevant ecological information that may support management actions on the SJG shellfish artisanal fishery.

Keywords: bio-optical properties, remote sensing, macronutrients, San José Gulf.

1. Introduction

Phytoplankton is the ocean autotroph for excellence. It is responsible for about 50% of global primary production (Field et al., 1998), a key component of the carbon cycle and a good indicator of environmental conditions (Smetacek and Cloern, 2008; Gregg et al., 2003). The phytoplankton community closely interacts with the other components of the marine ecosystems. Thus, it is crucial to understand all the factors that govern the dynamics of the phytoplankton communities that ultimately determine the primary production (Litchman and Klausmeier, 2008).

Many environmental forces drive the fluctuation of phytoplankton biomass (Cloern and Dufford, 2005; Longhurst, 1998; Margalef, 1978). Nutrients, temperature, solar radiation, stratification and grazing, and their interactions are the most important factors determining its fluctuations at seasonal scales. At the same time, eutrophication and climate change are more significant at inter-annual and decadal scales (Blauw et al., 2018; McQuatters-Gollop and Vermaat, 2011; Richardson and Schoeman, 2004). Climate change affects the thermal regimen in coastal waters and column stability, stratification, nutrient availability, dissolved oxygen, precipitations, and coastal runoff (Winder and Sommer, 2012).

To understand phytoplankton's spatial and temporal variability in a specific system, it is necessary to collect significant amounts of field data covering large areas. Still, satellite ocean colour technology and algorithm developments have open alternative and complementary ways to reach synoptic coverage of phytoplankton dynamics from local to global scales over long periods and to observe a broad range of other geophysical and biological variables (Krug et al., 2018, 2017; Blondeau-Patissier et al., 2014). Surface waters' temperature and detection of reflected light from the water, are the most frequently variables monitored by satellite sensors, providing relevant information on the physical and biological conditions of the marine systems (Gholizadeh et al., 2016).

The colour of the ocean mainly focuses on determining the concentration of chlorophyll-a (Chla), the main photosynthetic pigment, and therefore the most widely used proxy to study the variability of phytoplankton biomass (Huot et al., 2007). However, Chla retrieval is problematic in optically complex coastal waters, where dissolved organic matter (CDOM) and detritus are as important as phytoplankton (Blondeau-Patissier et al., 2014; Werdell et al., 2018, Delgado et al., 2021). The reflectance spectra of water masses greatly depend on the inherent optical properties (IOPs), resulting from the different concentrations of optically active components in seawater (Gordon et al., 1988). In the last years, the study of the IOPs has demonstrated to be one of the most robust tool to estimate phytoplankton properties from remote sensing data (Blondeau-Patissier et al., 2014; Kratzer and Moore, 2018; Aguilar Maldonado et al. 2019). The absorption by phytoplankton is one of the most important inherent optical properties of seawater, affecting the spectral reflectance of the ocean. Thus, this property reflects changes in phytoplankton biomass, phytoplankton types, and community structure (e.g., Bricaud et al., 2004; Sathyendranath et al., 2004).

The Patagonian Continental Shelf (PCS) has been described as one of the most productive areas of the world's oceans in terms of phytoplankton biomass (Rivas et al., 2006; Romero et al., 2006). In this region, the analysis of the spatio-temporal variability of Chla concentration through ocean colour satellite images allowed to characterize climatological regions (Andreo et al., 2016; Rivas et al., 2006; Glembocki et al., 2015; Williams et al., 2021) and quantify its primary production (Dogliotti et al., 2014; Segura et al., 2013; Lutz et al., 2010). Likewise, the performance of standard chlorophyll-a algorithms has been evaluated, observing an acceptable performance in open waters (Dogliotti et al. 2009) and very low in coastal ones (Williams et al., 2013; Delgado et al., 2019). Several absorption algorithms by phytoplankton have been evaluated in the optically complex waters of "El Rincón" (Argentina), observing an acceptable performance of the absorption by phytoplankton at 443 nm from GIOP model (r^2 = 0.48, BIAS 52%, Delgado et al., 2019). Contrarily, the estimation of phytoplankton biomass using standard absorption by Chla-sat in other areas of the Argentinean coastal waters has shown low performance as a proxy of phytoplankton biomass in these optically complex waters (r^2 = 0.15, BIAS 113%, Williams et al., 2013).

The San José Gulf (SJG) is a small and relatively shallow (mean depth 30 m, maximum 80 m) semi-enclosed basin located north of the PCS (between latitudes 42°14′ and 42°26′S). Its waters are connected through a narrow mouth (i.e., 6.9-km wide) in a N–S direction (SHN, Carta H214; Amoroso and Gagliardini, 2010) with those of the larger and deeper San Matias

Gulf (SMG). SJG is part of the Peninsula Valdés Protected Area, a natural reserve designated as a World Heritage Site and Biosphere Reserve by the United Nations Educational, Scientific and Cultural Organization (UNESCO) due to its importance for marine conservation. Nutrient-rich waters from the adjacent PCS, such as those from the Península Valdés (PV) frontal system, have been tracked in their passage through the southern region of SMG into SJG (Tonini et al., 2006; Gagliardini and Rivas, 2004; Rivas and Beier, 1990; Charpy and Charpy-Roubaud, 1980a; Carreto et al., 1974; Carreto and Verona, 1974), contributing to its high nutrient concentration and productivity (Charpy, et al., 1983; Charpy and Charpy-Roubaud, 1980b). These highly productive waters support an artisanal fishery mainly focused on the scallop *Aequipecten tehuelchus* (Orensanz et al., 2007; Amoroso et al., 2011) and of other species target of recreational fisheries (Venerus et al., 2008). As a result of the interaction between tidal circulation, the asymmetric northwest location of its narrow mouth, topography and geomorphology, two distinct hydrographic domains are generated in SJG: a highly vertically-mixed western domain (WD), and more stagnant eastern domain (ED) showing a strong vertical stratification during the warm season, thus promoting the formation of a thermal front between each other (Amoroso et al., 2011; Amoroso and Gagliardini, 2010; Gagliardini and Rivas, 2004). These two contrasting hydrographic domains are associated with differences in the mesozooplankton assemblages (Hernández-Moresino et al., 2017, 2014). There is a consistent spatial correlate between physical conditions of the water masses (SST, and bottom depth) and the mesozooplankton community structure (abundance, biomass, and slope of the size spectra), which should be also linked to the fluctuation of the phytoplankton biomass in the two hydrographic domains.

Hence, the main questions that prompted the present work are: (i) Do surface waters of the eastern and western domains of SJG and the neighbouring shelf present different seasonal variation patterns of phytoplankton biomass proxies and related bio-optical variables?; ii) How can the entire system be classified and understood based on the bio-optical properties?, and (iii) What are the main environmental factors driving phytoplankton dynamics in the SJG?

1. Materials and Methods

1.1. Study system

Based on the oceanographic characteristics of the area, a 15-year time series of satellite data on absorption by phytoplankton at 443 nm and other associated satellite variables described in the next section were analyzed, covering the northeastern coastal area of Peninsula Valdés (PV), south of the San Matías Gulf (SMG), and the entire San José Gulf (SJG, Fig. 1). Additionally, an exhaustive field sampling was carried out during the spring and summer seasons in the SJG with a particular setting at the beginning and the end of the thermal frontal system formation to get records of Chla, pH, temperature, redox potential, and nutrients concentration.

1.2. Remote sensing data

Images of absorption by phytoplankton (aphy at 443 nm, $aphy_{443}$, GIOP model, Franz and Werdell, 2010; Werdell et al., 2013), absorption by detritus plus coloured dissolved organic matter (adg at 443 nm, adg_{443}, GIOP model), monthly mean chlorophyll-a (Chla-sat, standard chlorophyll-a derived from the OC3M algorithm v2018), sea surface temperature (standard MODIS 11 µm, night, non-linear sea surface temperature algorithm NLSST vR2019.0), PAR (Photosynthetically Available Radiation, MODIS-Aqua_L3m_PAR v2018), and ZLEE (Euphotic depth, $Z_{1\%}$, Lee algorithm, MODIS-Aqua_L3m_ZLEE v2018, Lee et al., 2007) were used. Images with 4 Km spatial resolution, and covering the period January 2003–December 2018 were obtained from https://oceancolor.gsfc.nasa.gov/ (MODIS Mission page 2020 a, b, c, d, e).

For the first inspection, maps of climatological seasonal averages of SST, $aphy_{443}$, adg_{443}, Chla-sat, and $Z_{1\%}$ were calculated. Seasons were defined as follows: summer, from January to March; autumn, from April to June; winter, from July to September; and spring, from October to December.

After this first inspection and taking into consideration prior research in the area (Williams et al., 2018a, 2021; Amoroso and Gagliardini, 2010), the study system was partitioned into 5 windows: Península Valdés (PV, 9x9 pixels), Punta Norte (PN, 6x5 pixels), south of SMG (SSMG, 7x6 pixels), and western and eastern domains of SJG (WD and ED respectively, 4x3 pixels) (Fig. 1a). The inclusion of very coastal pixels in the considered windows was avoided.

Finally, climatology monthly mean images of SST, $aphy_{443}$, adg_{443}, Chla-sat, and $Z_{1\%}$ were generated for each window, averaging all scenes available for each month, on a pixel-by-pixel basis, obtaining a series of twelve climatological images. Climatology monthly mean images were obtained using SeaDAS software (version 7.5.3). The spatial resolution of the input images (4 km) was kept.

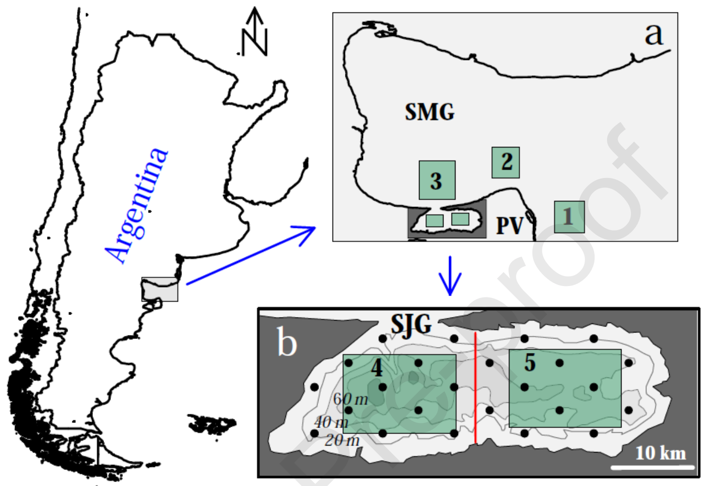

Figure 1: Location of the study area.(a) Selected windows for time series analyses of satellite data are showed in green boxes.(b) Locations of field sampling stations are indicated by black circles. Vertical red line in b shows the approximate location of the front that separates the Western and Eastern Domains with different hydrographic regimes (Amoroso and Gagliardini, 2010). Windows are numbered from 1 to 5: Península Valdés (PV), Punta Norte (PN), south of San Matías Gulf (SSMG), and western (WD) and eastern (ED) domains of San José Gulf (SJG).

1.3. Field sampling

Field sampling was conducted in waters of SJG, covering the entire gulf's area (Fig. 1b). A spatial grid was set, with 14 water samples obtained in September–November 2016 (spring), when vertical stratification begins to develop in the eastern hydrographic domain (ED), and with 22 water samples in March–April 2017 (summer–autumn), when it vanishes. The samples were collected using a Niskin water sampler, at three depths: near the surface, 10 m, and near the bottom.

Temperature, conductivity, salinity, redox potential, and pH were recorded in the field using a pre-calibrated multiprobe YSI556. Samples were kept cold until arrived to the laboratory. There, 1.5-2 l of each sample were filtered using 0.4 µm pore GF/F filters (Munktell®). Filters and 200 ml PET bottles with filtered water were stored in the freezer at −20°C for further analyses of phytopigments and macronutrients.

Chlorophyll-a (Chla) and pheophytin (Pheo) were measured with a Turner Designs fluorometer after extraction with 90% acetone (Strickland and Parsons 1972). Calibration was performed using a pure chlorophyll standard (*Anacystis nidulans* algae — Sigma-Aldrich). The macronutrients such as nitrate (NO_3^-) + nitrite (NO_2^-), referred hereafter as dissolved inorganic nitrogen (DIN), phosphate (PO_4^{3-}) referred as dissolved inorganic phosphorous (DIP), and silicic acid ($Si(OH)_4$) or dissolved silica (DSi) were determined by colorimetric methods using a Skalar San Plus autoanalyzer (Skalar Analytical® V.B., 2005 a, b, c).

1.4. Statistical analysis of oceanographic and bio-optical variables

Principal Component Analysis (PCA) was applied to the climatological data set to classify each sampling window within the study area, grouping those with similar monthly variability patterns following methodology described by Gonzalez-Silvera et al. (2004). Thus, each window was treated as a variable (n = 5) and each month as the object describing such variable (n= 192, 2003-2018). The matrix (5x192) was transformed into a correlation matrix (192x192) that was used as input for PCA calculations. Components with cumulative variance greater than 90% were taken as significant and locations were classified according to the correlation matrix between PCA results and time series location.

Monthly climatological series of $aphy_{443}$ and Chla-sat data for each sampling window were adjusted to an annual plus semi-annual cycle by the least-squares data fitting (Eq. 1, Espinosa-Carreon et al., 2004) to obtain their stationary signal:

$$\text{Data-sat} = \text{Data-sat}_0 + T_1 \cos\left(w(t - t_0)\right) + T_2 \cos 2\left(w(t - t_{00})\right) \quad \text{(Eq. 1)},$$

where Data-sat_0 is the mean temporal value of $aphy_{443}$ or Chla-sat, T_1 is the annual harmonic amplitude, T_2 is the semi-annual harmonic amplitude, w is the frequency (w = 2π/12 months), t_0 and t_{00} are the annual and semi-annual harmonic phases, respectively. The fit of the data to a mean plus annual and semi-annual harmonics model explains the total variance (r^2_{a+s} = 1, a = annual, s = semi-annual). The contribution of each harmonic (annual and semi-annual) to the cycle was determined by fitting monthly climatological data to each harmonic separately (second and third terms of Eq. 1, respectively, as stated in Williams et al. (2018a).

Pearson's correlation coefficient (r) was applied between pairs of bio-optical variables to measure the association between the two variables considered. Kriging interpolation method was used in order to map the spatial distribution of chlorophyll-a in the field.

2. Results and discussion

2.1. Spatial and seasonal variability of SST, $aphy_{443}$, and $Z_{1\%}$.

The spatial distribution of the climatological maps of SST was relatively uniform in autumn and winter (Fig. 2a and b). In the former, the temperature was around 15°C, and in the latter it was 11-12°C. In spring and summer (Figure 2c and d), the SST distribution showed spatial heterogeneity: lower values were observed to the east and north of PV and in the western domain of SJG (spring 11-12° C; summer 15°C) compared to the rest of the study area (spring 13-14°C, summer 18-19 °C).

The $aphy_{443}$ showed values of 0.025-0.030 m^{-1} in the east and northeast of PV and the western domain of SJG in autumn (Fig.2e). In winter, a decrease was observed in the SJG and southern SMG (0.016-0.020 m^{-1}, Fig. 2f). The $aphy_{443}$ increased in spring, showing the highest annual values in almost the entire area (including the eastern domain of the SJG, 0.025-0.068m^{-1}), lower values to the north of PV, and the WD of the SJG (0.025 mg m^{-1}, Fig. 2g). Finally, the spatial distribution of $aphy_{443}$ in summer was similar to that of spring but with lower values (0.010-0.045 m^{-1}, Fig. 2h).

The depth of the euphotic zone ($Z_{1\%}$) showed spatial heterogeneity and similar distribution patterns during all the year (Fig. 2, i to l): lower values were observed to the east and northeast of PV (20-22 m), mainly in autumn and winter, while $Z_{1\%}$ increased towards the south of GSM (28-32 m). In the case of GSJ, slight differences between domains were observed in spring and summer (Fig. 2, k and l), with higher values in the eastern than in the western domain, resembling that observed with the SST patterns and that can be associated with the thermocline formation in this domain.

In general terms, the spatial pattern of SST, $aphy_{443}$, and $Z_{1\%}$ in spring and summer can be explained by the development of a tidal front located at the mouth and to the south of SMG (Pisoni et al., 2015; Rivas and Pisoni, 2010; Gagliardini et al., 2004; Piola and Scasso, 1988). The tidal front separates the mixed waters in shallow sectors (less than 70 m) on the adjacent continental shelf from the deeper waters that tend to stratify into SMG (Williams et al., 2013). Thus, the coastal waters from PV present lower temperatures, higher $aphy_{443}$ values and shallower $Z_{1\%}$ compared to the surrounding waters due to mixing caused by tidal currents and energy dissipation in the area (Palma et al., 2004). The SST and $Z_{1\%}$ maps suggest the entry of water from the continental shelf through the south of SMG to the western portion of the GSJ.

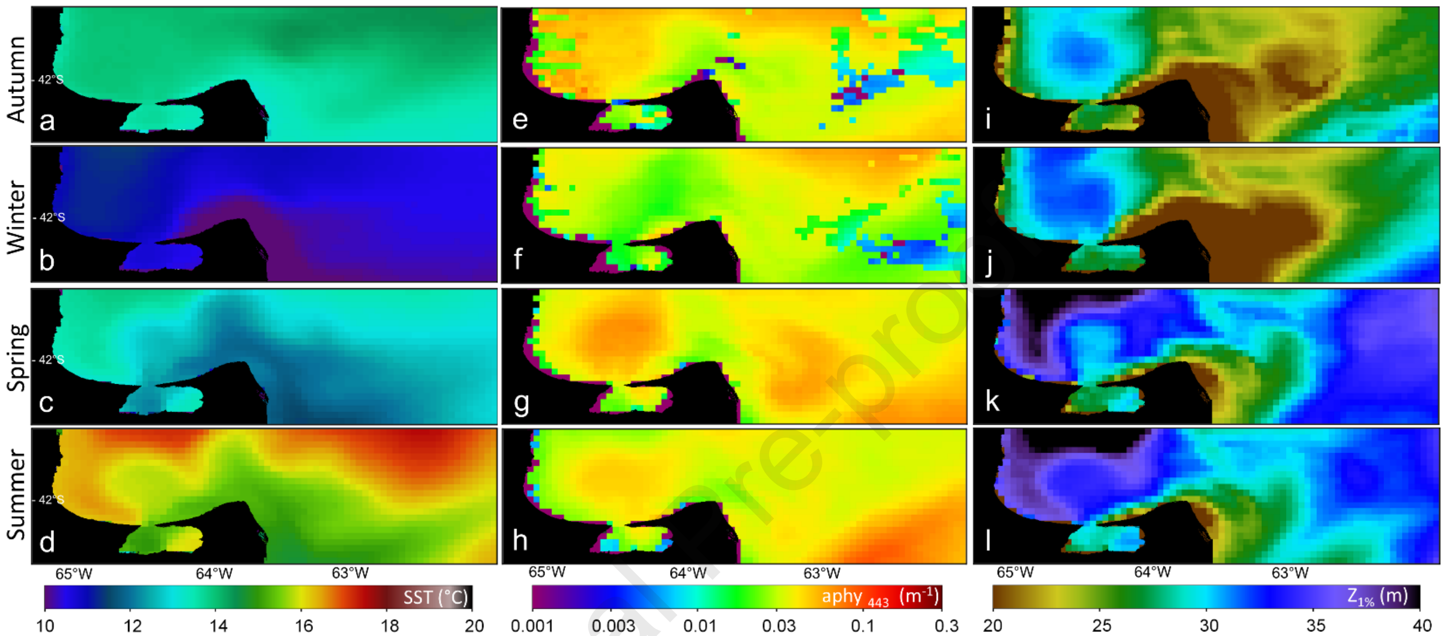

Figure2: Climatological maps of Sea surface temperature (SST; a-d), absorption by phytoplankton at 443 nm ($aphy_{443}$; e-h) and depth of euphotic zone ($Z_{1\%}$; i-l) expressed by seasons. The values are expressed as average from year 2003 to 2018.

2.2. Principal Component Analysis (PCA) of $aphy_{443}$, adg, Chla-sat and $Z_{1\%}$ temporal variability

Performing the PCA for each bio-optical variable, including the 5 sampling windows, they yielded 3 main components, explaining more than 90% of the variance in all cases (Fig. 3). The analysis using $aphy_{443}$ associated SJG (WD and ED) with SSMG supported by PC_1 ($r > 0.69$), while PN and PV were represented by PC_2 ($r > -0.72$). This pattern was also observed by Chla-sat parameter, where the SJG domains and the southern SMG were also represented by PC_1 ($r > 0.85$), whereas PN and PV were represented by PC_1 and PC_2 (0.69 and 0.64, respectively). The PCA results using adg are not concluding, however, it is evidenced a slight association between PV and PN on the one hand, and between the domains of SJG on the other hand, with SSMG in the middle, similar to the grouping defined by $aphy_{443}$ and Chla-sat. In the cases of the depth of the euphotic zone ($Z_{1\%}$), it was observed that the ED together with SSMG, PN and PV correlate mainly with PC_1 (>0.64). On the contrary, the WD window presents a particular behaviour associated with PC_3 (0.96).

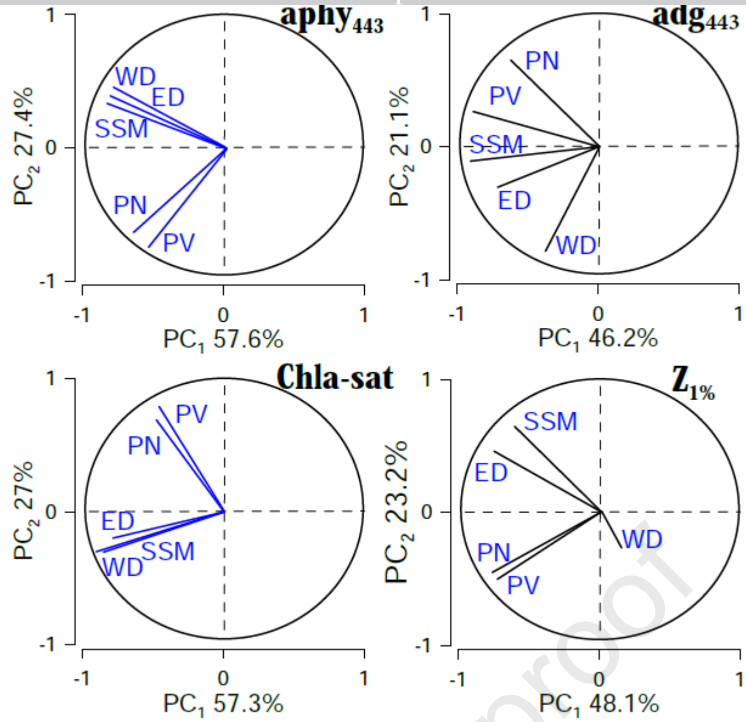

Figure 3: Plots for the first and second factors for the PCA regarding bio-optical variables.

2.3. Climatological annual cycle of PAR, $Z_{1\%}$, $aphy_{443}$, Chla-sat and adg_{443}.

The PAR cycle showed a typical annual signal evidenced with high percentage of variance explained by the annual harmonic (Williams et al., 2018a), with minimum values from May to July (15.41 to 13.51 E m^{-2} d^{-1}) and maximum values from November to January (54.86 to 60.12 E m^{-2} d^{-1}). In general, the annual cycle of $Z_{1\%}$ (euphotic depth) also showed strong annual signal and positive correlation with PAR and SST, with minimum mean values in June (24 m), and maximum values from December to February (~ 30 m). High correlation between $Z_{1\%}$ and PAR series were evidenced in PV and PN windows (r^2> 0.9), as well as in the ED (r^2 = 0.67). This slightly lower correlation in the ED can be explained by the increase in $Z_{1\%}$ during July and August (Figure 3, e), probably due to the decrease in the suspended organic matter, as a consequence of the low biological activity and the sinking of particles towards the bottom. Conversely, SSMG and the WD of SJG reveal a low temporal variability (SSMG = 31.32 ± 1.45 m and WD = 27.54 ± 0.87 m) and a lack of correlation with the PAR cycle. They presented the lowest or null relationship between these parameters (0.32 and -0.10), suggesting that PAR effect on $Z_{1\%}$ is masked by other variables such as suspended materials from land and sea bottom sources all year round.

The $aphy_{443}$ for PN and PV windows showed little annual variability and a moderated peak in November (Fig. 3a and b), showing a good fit to the unimodal function (r^2 = 0.67 and 0.70 respectively, Supplementary Materials, Table I). The Chla-sat estimated for PN and PV windows also showed little annual variability and a moderated peak in November (Fig. 3, a and b), showing a good fit to the unimodal function in the case of the PV and no significant fit to any harmonic function in the case of PN (r^2 = 0.85 and 0.33 respectively, Supplementary Materials, Table II). This low annual variability can be explained by the high tidal energy flow that prevents the stratification of the water column (Tonini and Palma, 2017; Palma et al., 2004). In the case of the SSMG and GSJ windows, they showed broad annual variability with a high peak also in November ($aphy_{443}$ = 0.04- 0.08 m^{-1}, Chla-sat = 3.46-4.39 mg m^{-1}) and low values in winter (August, 0.02 m^{-1}; 1.00 mg m^{-1}), fitting to the unimodal function using either $aphy_{443}$ or Chla-sat parameters (r^2 ~ 0.7, Supplementary Materials, Table I and II), in agreement with previous studies using shorter time series (2003-2009, Williams et al., 2018a, 2013). Particularly in the SSMG window, moderate values there were sustained during summer-early autumn (from February to April: 0.04± 0.005 m-1; 1.33±0.01 mg m^{-1}) probably due to the continuous injection of nutrients leading by the interaction of tidal currents with the topography (Williams et al., 2013, 2021). This feature can be observed to some extent within SJG also explained by a permanent income of nutrient through the mouth.

The Chla-sat annual cycle in SJG has already been characterized by an annual harmonic function with relatively high values in spring-summer (Williams et al., 2018a). As a novelty, the present work highlights the differences between the western and eastern hydrographic domains supported by $aphy_{443}$ as a proxy for phytoplankton biomass. Although the $aphy_{443}$ and Chla-sat annual cycles are mainly explained by the annual harmonic function, the ED presents a significant contribution of the semiannual harmonic function given by the absorption by $aphy_{443}$ (r^2 = 0.71, Supplementary Materials, Table II). The ED showed two maximums: the first from October to December (0.04± 0.005 m^{-1}), and the second in March-May (0.04± 0.0006 m^{-1}), gradually decreasing until July (0.03 m^{-1}), similar to that of temperate areas biomass phytoplankton cycle with seasonal stratification of the water column (Mann and Lazier et al., 2006).

The climatological annual cycles of the bio-optical variables showed a general pattern of higher absorption by adg_{443}than that by $aphy_{443}$ (~ 0.09 and 0.03 m^{-1}, respectively, Fig. 3). The relatively much higher absorption by adg_{443} is a characteristic optical feature alongside coastal and shallow waters with strong hydrodynamics (Werdell et al., 2018; Blondeau-Patissier et al., 2014). Adg may originate either from the degradation of phytoplankton cells and other organic particles from water or terrestrial sources (Lutz et al., 2016; IOCCG, 2000). Usually, the former accounts for a higher percentage of adg in the open ocean, while the latter dominates in coastal, estuarine, and inland waters (Zhang et al., 2013; Bricaud et al., 1981), with contribution from bottom sediments during storm-driven suspension events (Boss et al., 2001).

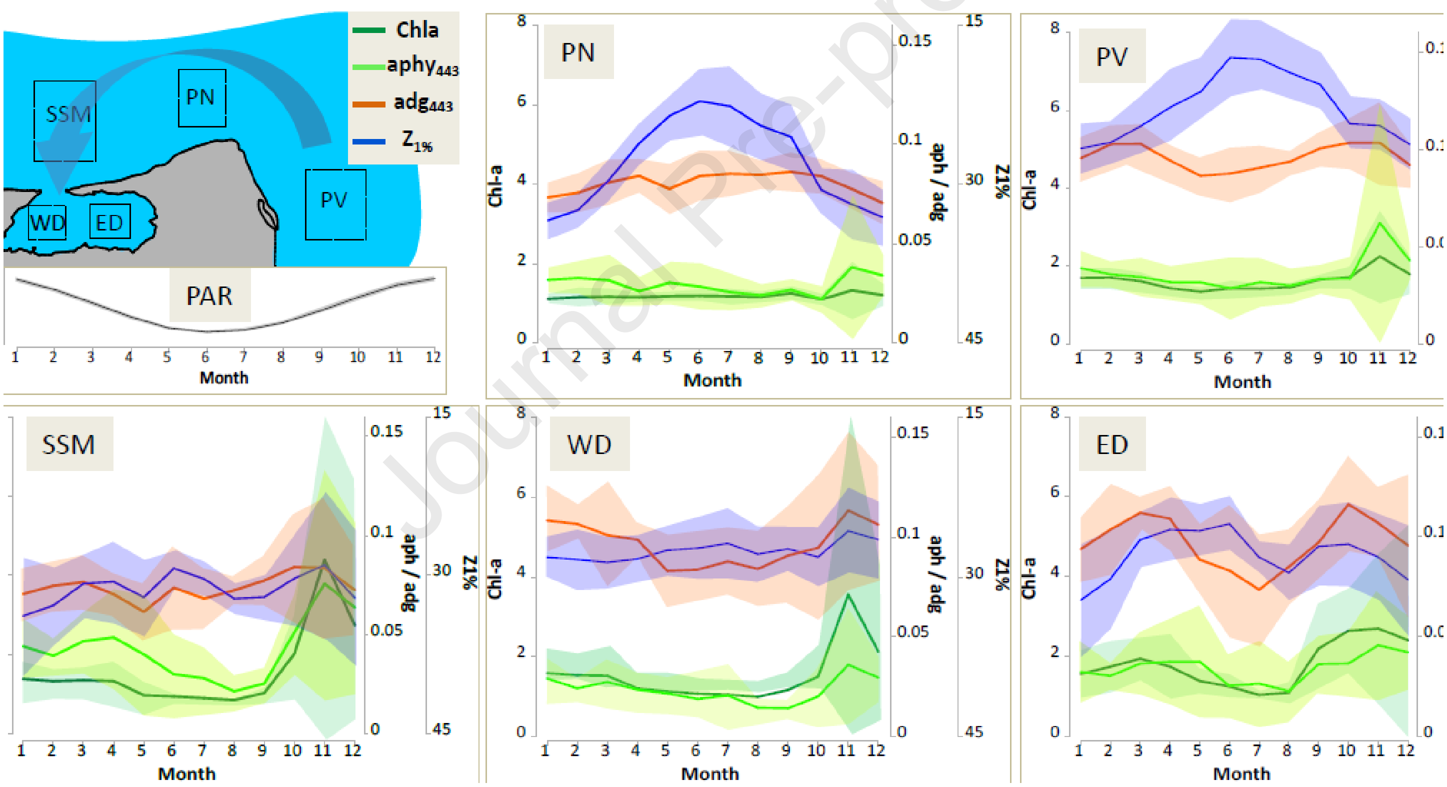

Figure 4: The annual cycle of bio-optical variables in the upper layer estimated by satellite remote sensing. Blue arrow into the map schematizes the flow of the water masses from the platform (from Península Valdés or PV) into San José Gulf (GSJ), western and eastern domains (WD and ED), flowing through Punta Norte (PN) and the south of San Matías Gulf (SSMG). PAR plot shows the solar irradiance cycle, equal for all the areas under study. Chlorophyll-a is expressed in mg m^{-3}, adg_{443} and $aphy_{443}$ in m^{-1}, $Z_{1\%}$ in –m, and PAR in E m^{-2} d^{-1}).

2.4. Interaction of bio-optical variables

The absorption by phytoplankton ($aphy_{443}$) is closely related to the Chla-sat variability, regardless of its relatively low values compared to cdom + detritus (adg_{443}). This association was the highest outside of GSJ (SSMG, PN, and PV, r^2 ~ 0.8, Table I), indicating similar annual variability between $aphy_{443}$ and Chla-sat. It decreased in the GSJ domains (r^2 ~ 0.6, Table I), being even higher than the relationship in the ED. It is important to note the low correlation between $aphy_{443}$ and adg_{443}, ruling out any covariance between both variables (Table I).

The correlation between the depth of the euphotic zone ($Z_{1\%}$) with Chla-sat, $aphy_{443}$, and adg_{443} were low in some cases (mainly in SJG) and near-zero in others (mainly in PV and PN), with slightly higher values in SSMG than in SJG (r^2<-0.56, Table I). These weak and negative relationships in SSMG and SJG likely respond to an increment of the phytoplankton biomass (estimated as Chla-sat and $aphy_{443}$) and detritus and dissolved organic matter (adg_{443}), both absorbing light through the water column in spring and summer. On the other hand, the absence of correlation between $Z_{1\%}$ and the bio-optic parameters in PV and PN areas would indicate that other factors that affect the low penetration of PAR throughout the year, such as inorganic suspended sediments (Capuzzo et al., 2015).

The waters in SJG display complex optical patterns, where the absorption of light is dominated by detritus and cdom instead of the phytoplankton processes of the water column (Williams et al., 2018b; Morel and Prieur, 1977 and references therein). Allochthonous material coming from the continent (runoff, atmospheric dust, landslides, among others) likely governs the IOPs in this enclosed basin (Zhang et al., 2013; Bricaud et al., 1981).

Table I: Correlations between the main bio-optical variables. Values > 0.6 are highlighted in bold.

Pair-correlations	PV	PN	SSM	WD	ED
$aphy_{443}$ vs Chla-sat	**0.88**	**0.79**	**0.82**	**0.63**	0.55
$aphy_{443}$ vs adg_{443}	0.17	-0.41	0.35	0.22	0.05
$aphy_{443}$ vs $Z_{1\%}$	-0.06	-0.04	**-0.69**	-0.42	-0.50
adg_{443} vs $Z_{1\%}$	0.08	-0.44	-0.56	-0.07	-0.46
adg_{443} vs Chla-sat vs	0.46	0.14	**0.65**	0.40	**0.60**
Chla-sat vs $Z_{1\%}$	-0.35	-0.05	**-0.61**	-0.52	-0.54

2.5. Water column chlorophyll-a patterns in SJG

Results from field sampling conducted at the beginning and the end of the frontal system formation in SJG suggest that the spring sampling did not coincide with the bloom period since the Chla values were low for the entire SJG. On the other hand, the second phytoplankton peak estimated by satellite data in the ED was reflected by the results of the summer sampling.

The field data in the three strata of the water column shows some particularities to consider (Fig. 5). High Chla values were found in the north coast of the ED during the two sampling seasons: in the surface sample in spring and at all depths in summer. High Chla concentrations were also found in the bottom of the southeast coast for both seasons. In addition, moderate Chla values were observed in the frontal zone in summer. In terms of pheopigments (data not shown), they were always low (~ 0.1 mg m^{-3}) except for the very high values in the bottom of the southeast coast, both in spring and summer (2.5 and 1.5 mg m^{-3}, respectively). These two singular events of high Chla contents in the north of the ED and of high pheopigment contents in the bottom of the southeast coast of the ED suggest particular conditions of these coastal areas. Previous work on sediment circulation patterns (Hernández Moresino et al., 2019) indicated that the prevailing southward winds in spring and summer would generate a surface circulation of the water masses in the same direction.

Contrarily, the analysis of transport vectors carried out in the same work showed a northward trend of sediment transport in summer. Summarizing these results and considering water bodies act as a continuous fluid, the authors suggest that prevalent southward winds generate an upwelling event in the northern coasts of the ED during the spring and summer. Surface waters driven southward, leave a space occupied by reach-nutrient bottom waters, evidenced by the Chla registered in the entire water column in spring and summer. In this sense, in the southern coasts of the ED there might be a downwelling event caused by the surface water masses that come from the north and force the local waters to sink, evidenced by the high levels of pheopigments and Chla in the bottom waters of the area also in spring and summer.

Chla-field maps were constructed and compared with those obtained from satellite data for the same dates. No clear similarities were observed between both sets of data (Fig. 1, supplementary materials). Nor a clear correlation fit observed when both data sources were contrasted (r^2 = 0.11-0.27; n = 8-14). This low correlation could be explained by the complexity of the optical characteristics in the gulf (high absorption of cdom + detritus), as well as by the intrinsic differences between each estimation method (spatial and temporal coverage of satellite images vs. interpolation of *in-situ* data, the time difference between estimates in a complex system, among others).

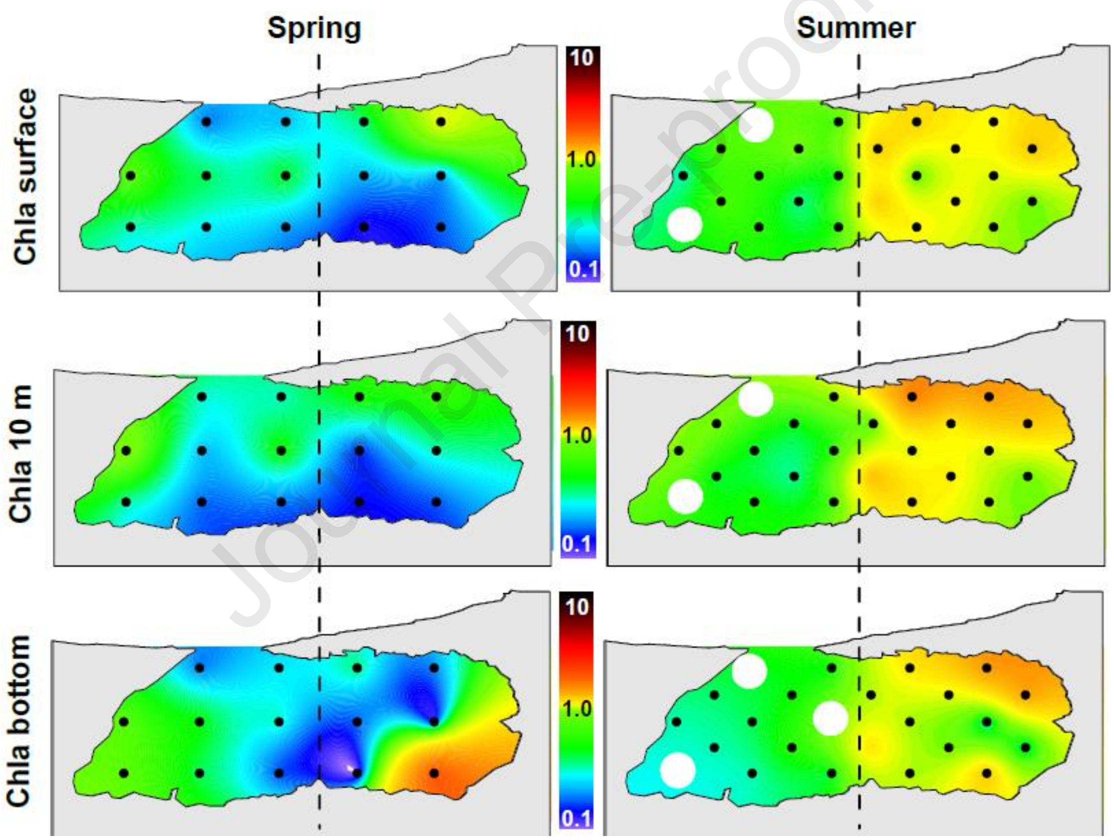

Figure 5: Field chlorophyll-a maps by stratum (surface, 10 m, and near bottom). Dashed vertical lines divide the two sampling time for each sampling season (spring sampling: 28/09/16 ED and 09/11/16 WD; summer sampling: 16/03/17 ED and 27/04/17 WD). White circles represent missing data.

2.6. Vertical profiles of *in situ* environmental hydrographic variables

Depth profiles of some environmental variables were used to identify differences between the hydrographic domains into SJG (Fig. 6). A marked increase in temperature was observed in both parts from spring to summer, with high values in the ED, which is consistent with previous studies (Amoroso et al., 2011). However, the temperature profiles did not detect the occurrence of the water column stratification of the ED in the present study. The redox potential showed an apparent decrease during summer in both domains, which suggests a critical oxygen consumption during the warm season due to the zooplankton proliferation, the high bacterial degradation activity, and a consequence of an increase in phytoplankton biomass. On the contrary, the pH values remained constant and no differences were observed between seasons.

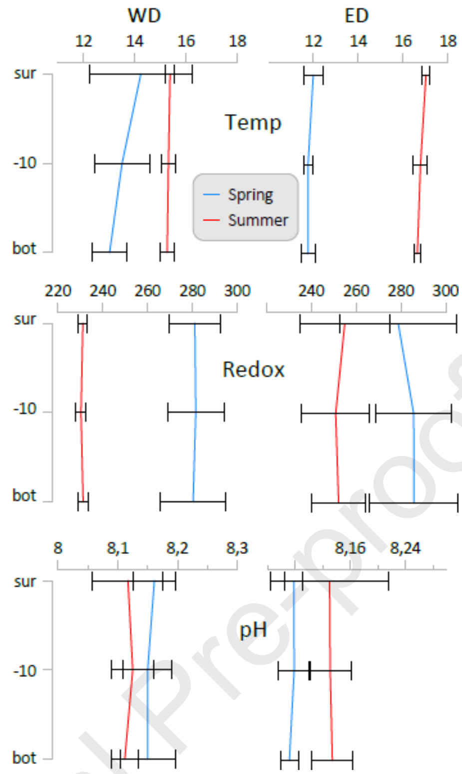

Figure 6: Relevant environmental variables profiles from in situ data in the two domains of SJG. Sur: surface. Bot: bottom. Horizontal bars represent the mean value and standard deviations of all available data.

Regarding the macronutrient profiles (Fig. 7), WD spring samples showed lower values of all parameters than their summer counterparts, suggesting that the spring sampling was conducted after an increase of phytoplankton biomass event (Fig. 4, WD). Conversely, ED samples only showed lower values of dissolved inorganic nitrogen (DIN) in summer. Low values of DIN in the ED summer samples show a significant consumption of this macronutrient, close to being undetectable, indicating that this sampling was carried out at the end or after the second phytoplankton bloom (Fig. 4, ED).

In marine environments, the criteria of absolute nutrient limitation thresholds for phytoplankton growth (Justić et al., 1995) suggest values of DIN = 1 µmol L^{-1}, DIP = 0.1 µmol L^{-1}, and DSi = 2 µmol L^{-1}. According to that, DIN is the only macronutrient that can restrict phytoplankton growth in the ED in summer. No nutrient limitation was found regarding the other two macronutrients with values above their absolute criteria, except for a probably slight DSi-limitation in some stations for both seasons (DSi>1.4 µmol L^{-1}).

Nutrients affect and determine the phytoplankton growth according to the ecology strategies. Its distribution is disparate and terrestrial runoff, or upwelling events are the main hotspots (Wang and Gao, 2020; Roelke and Spatharis, 2015; Buyukates and Roelke, 2005). Nutrient pulse will favour the proliferation of fast-growing species (r-strategists or opportunists). In contrast, species with a higher affinity for limiting nutrients (k-strategists or gleaners) will have the competitive advantage during the nutrient depletion period, which occurs before the next nutrient pulse (Papanikolopoulou et al., 2018; Sommer, 1989; Kilham and Kilham, 1980). In this context, the rapid growth of r-strategist species proliferates in spring when optimal light and nutrient conditions. They consume part of the macronutrients in the WD and almost all the nitrogenous products in the ED. The persistence of the moderated concentration of phytoplankton during the summer in the ED would respond to the growing of k-strategist species in the upper mixed layer until the next nutrient pulse in March when the thermocline disrupts, favouring a second seasonal increase of phytoplankton biomass of r-strategist.

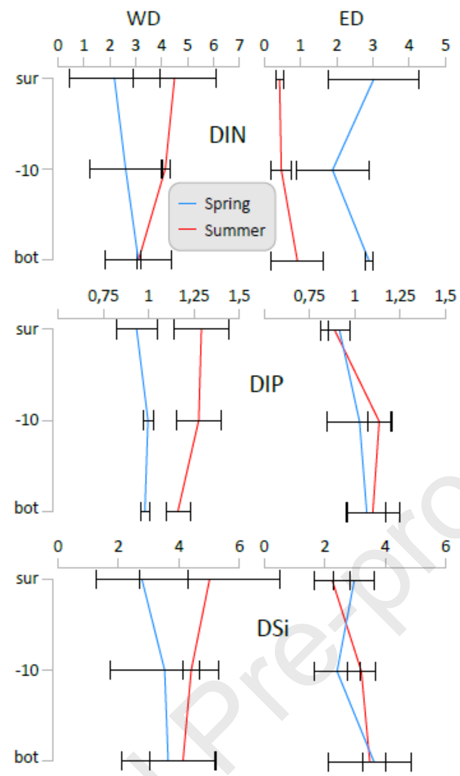

Figure 7: Macronutrients profiles from in situ data in the two domains of SJG. DIN: dissolved inorganic nitrogen. DIP: dissolved inorganic phosphorous. DSi: dissolved silica. Sur: surface. Bot: bottom. Horizontal bars represent mean value and standard deviation of all available data.

3. Conclusions

The seasonal variability of $aphy_{443}$ as a proxy for phytoplankton biomass shows that the system describes a classic temperate environment (Mann and Lazier, 2006), with high $aphy_{443}$ values in spring, decreasing during summer, and reaching low values in autumn and winter. The availability of light and nutrients explains maximums found in SSMG and SJG in spring before summer. Remarkably, the ED of SJG presents a second maximum in the late summer and autumn, associated with the erosion of the thermocline and the reinjection of nutrients to the upper layer. In contrast, moderate and low variability values of $aphy_{443}$ in PN and a weak peak in the northeast of PV are explained by low light penetration in the water column resulting from suspended sediments associated with turbulence produced by strong tidal currents in shallow waters.

A graphical synthesis of the conceptual framework of the SJG system (Fig. 8) shows that in the WD, the water column remains vertically mixed throughout the year, given the strong tidal currents that favour the suspension of particulate material absorbing light and avoiding the increase of $Z_{1\%}$ during the warm season. The high peak of phytoplankton biomass in this domain in spring decreases rapidly, probably associated with a combination of ecological factors of phytoplankton populations with fast growth rates: r-strategist with a fast rate of nutrients consumption and/or self-shading that limit the light penetration (Holligan et al., 1984). However, an increase in the stratification of the water column during the warm season in the more stagnant ED and the rise in light associated with the deeper euphotic zone, favour an earlier increase in the spring biomass of phytoplankton. This event persists longer and slowly decreases until the second increase in late summer, likely explained by the stability disruption of the water column and the re-injection of nutrients into surface water. The phytoplankton populations growing in the ED probably differ from those in the WD, with lower growth rates typical of k-strategist.

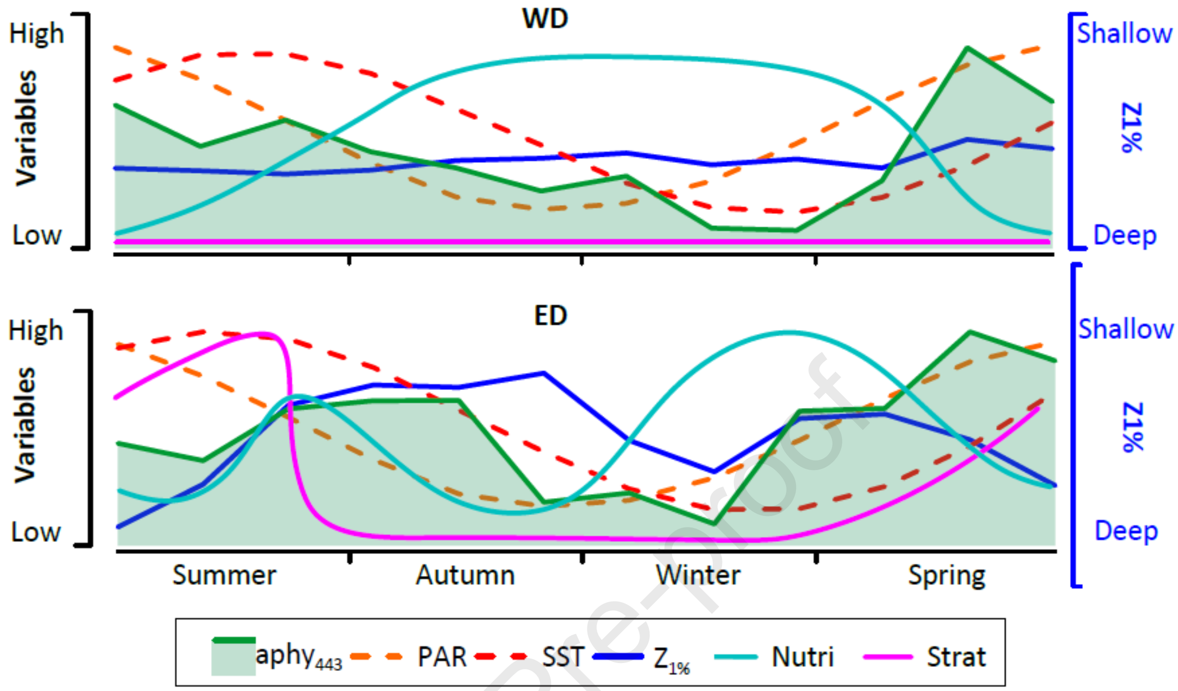

Figure 8. Conceptual framework of the annual cycles of sea surface phytoplankton dynamics (based on $aphy_{443}$ satellite estimation) along with related critical variables in the western and eastern domains of SJG.

The environmental conditions during the formation of the thermal front in SJG are summarized in detail in Figure 9. In both seasons, a water mass from the adjacent continental shelf enters SJG, as evidenced by the low SST and $Z_{1\%}$ values in the northeast of PV, SSMG, and the WD of SJG. As expected, the increase in solar radiation that reaches the upper layer of the water column during spring and summer generates a deeper penetration of light into the water column, promoting the growth of phytoplankton. The WD of the SJG presents particular bio-optic characteristics associated with strong hydrodynamics and a large amount of suspended material that shortens the annual variability of $Z_{1\%}$. Still, a high spring bloom in the WD allows concluding that phytoplankton can grow even in turbulent waters due to the high levels of nutrients that mostly come from external sources. On the other hand, the more isolated and seasonal stratified ED can uptake nutrients from the adjacent WD and local decomposers from the bottom sediments.

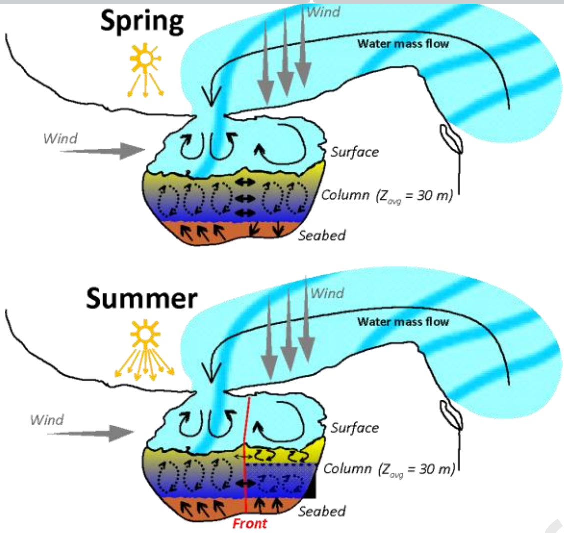

Figure 9. Schematic diagram of the main environmental processes during the frontal system formation in SJG.

Therefore, this work concludes that the nutrient (mainly DIN) and light regimes are the main drivers of the phytoplankton dynamics in the area. The annual light cycle affects the stability/stratification processes of the water column in the ED and, therefore, the availability of nutrients in the upper layer. In contrast, tidal currents prevent stratification in the WD throughout the year. These two counteracting hydrographic domains promote the formation of the thermal frontal system into SJG. Notably, the predominant southward winds during the warm season recorded in previous work (Hernández-Moresino et al., 2019) seem to be responsible for a vertical loop in the north-south direction, which produces an upwelling-downwelling structure in the ED and deserves further attention. All the information in this work lays the foundation for future ecological studies within this system that supports an important shellfish fishery, tourism, and ecosystem services in the Patagonian region.

Funding

This study was supported by Universidad Nacional de la Patagonia San Juan Bosco by a research project (grant number 318, 2018 to RHM); and the National Agency for Scientific and Technological Promotion of Argentina (ANPCyT, PICT 2014–1498 to RHM).

Acknowledgments

The authors thank the Ocean Biology Processing Group (Code 614.2) at the GSFC, Greenbelt, MD20 771, for the distribution of the ocean colour data. Sediment samples were collected in the framework of a provincial permit (Resolution N◦ 352/16 MT to RHM). Sample analyses were conducted at the Laboratory of Chemistry Oceanography and Water Pollution (LOQyCA CESIMAR-CONICET). We are grateful to F. Paparazzo, R Gonçalves, F. Quiroga, and F. Irigoyen for their assistance in field work. We gratefully acknowledge Dr. Pedro J. Barón for its comments on an earlier version of the manuscript. Also thanks to the anonymous reviewers for valuable comments that greatly improved the Ms.

4. References

Aguilar-Maldonado, J.A., Santamaría-del-Ángel, E., Gonzalez-Silvera, A., Sebastiá-Frasquet, M.T., 2019. Detection of Phytoplankton Temporal Anomalies Based on Satellite Inherent Optical Properties: A Tool for Monitoring Phytoplankton Blooms. Sensors, 19(15), 3339.

Amoroso, R.O., Gagliardini, D.A., 2010. Inferring complex hydrographic processes using remote-sensed images: turbulent fluxes in the Patagonian gulfs and implications for scallop metapopulation dynamics. Journal of Coastal Research, 26(2 (262), 320-332.

Amoroso, R.O., Parma, A.M., Orensanz, J.M., Gagliardini, D.A., 2011. Zooming the macroscope: medium-resolution remote sensing as a framework for the assessment of a small-scale fishery. ICES Journal of Marine Science, 68(4), 696-706.

Andreo, V.C., Dogliotti, A.I., Tauro, C.B., 2016. Remote sensing of phytoplankton blooms in the continental shelf and shelf-break of Argentina: spatio-temporal changes and phenology. IEEE Journal of Selected Topics in Applied Earth Observations and Remote Sensing, 9(12), 5315-5324.

Blauw, A.N., Benincà, E., Laane, R.W., Greenwood, N., Huisman, J., 2018. Predictability and environmental drivers of chlorophyll fluctuations vary across different time scales and regions of the North Sea. Progress in Oceanography, 161, 1-18.

Blondeau-Patissier, D., Gower, J.F., Dekker, A.G., Phinn, S.R., Brando, V.E., 2014. A review of ocean color remote sensing methods and statistical techniques for the detection, mapping and analysis of phytoplankton blooms in coastal and open oceans. Progress in oceanography, 123, 123-144.

Boss, E., Pegau, W.S., Zaneveld, J.R.V., Barnard, A.H., 2001. Spatial and temporal variability of absorption by dissolved material at a continental shelf. Journal of Geophysical Research: Oceans, 106(C5), 9499-9507.

Bricaud, A., Claustre, H., Ras, J., Oubelkheir, K., 2004. Natural variability of phytoplankton absorption in oceanic waters: Influence of the size structure of algal populations. Journal of Geophysical Research: Oceans, 109(C11).

Bricaud, A., Morel, A., Prieur. L., 1981. Absorption by dissolved organic matter of the sea (yellow sub- stance) in the UV and visible domains. Limnology and Oceanography, 26(1), 43–53.

Buyukates Y, Roelke D., 2005. Influence of pulsed inflows and nutrient loading on zooplankton and phytoplankton community structure and biomass in microcosm experiments using estuarine assemblages. Hydrobiologia, 548, 233–249.

Capuzzo, E., Stephens, D., Silva, T., Barry, J., Forster, R.M., 2015. Decrease in water clarity of the southern and central North Sea during the 20th century. Global Change Biology, 21, 2206–2214.

Carreto, J.L., Casal, A.B., Laborde, M.A., Verona, C.A., 1974. Fitoplancton, pigmentos y condiciones ecologicas del Golfo San Matías, Informe Comisión de Investigaciones Científicas Provincia de Buenos Aires, 10, 49-76.

Carreto, J.I., Verona, C.A., 1974. Fitoplancton, pigmentos y condiciones ecológicas del golfo San Matías I. Campaña SAO I (marzo 1971). Comisión de Investigaciones Científicas Provincia de Buenos Aires. Informe, 10, 1-22.

Charpy, L., Charpy-Roubaud, C.J., 1980a. La production primaire des eaux du Golfe San Jose (Peninsule Valdes, Argentine). II. Populations phytoplanctoniques et composition du seston. Hydrobiologia, 75, 215-224.

Charpy, L., Charpy-Roubaud, C.J., 1980b. La production primaire des eaux du Golfe San Jose (Peninsule Valdes, Argentine). III. Estimation de la production phytoplanctonique annuelle. Hydrobiologia, 75, 225-229.

Charpy-Roubaud, C.J., Charpy, L.J., Maestrini, S.Y., 1983. Nutrient Enrichments of Waters of "Golfo de San Jose" (Argentina, 42 °S), Growth and Species Selection of Phytoplankton. Marine Ecology, 4(1), 1-18.

Cloern, J.E., Dufford, R., 2005. Phytoplankton community ecology - Principles applied in San Francisco Bay. Marine Ecology Progress Series, 285, 11-28.

Delgado, A.L., Guinder, V.A., Dogliotti, A.I., Zapperi, G., Pratolongo, P.D., 2019. Validation of MODIS-Aqua bio-optical algorithms for phytoplankton absorption coefficient measurement in optically complex waters of El Rincón (Argentina). Continental Shelf Research, 173, 73-86.

Delgado, A.L., Pratolongo, P.D., Dogliotti, A.I., Arena, M., Celleri, C., Cardona, J.E.G., Martinez, A. (2021). Evaluation of MODIS-Aqua and OLCI Chlorophyll-a products in contrasting waters of the Southwestern Atlantic Ocean. Ocean and Coastal Research, 69, 1–6.

Dogliotti, A. I., Lutz, V. A., Segura, V., 2014. Estimation of primary production in the southern Argentine continental shelf and shelf-break regions using field and remote sensing data. Remote sensing of environment, 140, 497-508.

Espinosa-Carreon, T.L., Strub, P.T., Beier, E., Ocampo-Torres, F., Gaxiola-Castro, G., 2004. Seasonal and interannual variability of satellite-derived chlorophyll pigment, surface height, and temperature off Baja California. Journal of Geophysical Research: Oceans, 109(C3).

Field, C.B., Behrenfeld, M.J., Randerson, J.T., Falkowski, P., 1998. Primary production of the biosphere: integrating terrestrial and oceanic components. Science, 281, 237–240.

Franz, B.A., Werdell, P.J., 2010. A generalized framework for modeling of inherent optical properties in ocean remote sensing applications. Proceedings of Ocean Optics, Anchorage, Alaska, 27, 1-13.

Gagliardini, D.A., Rivas, A.L., 2004. Environmental characteristics of San Matías Gulf obtained from LANDSAT-TM and ETM+ data. Gayana (Concepción), 68(2), 186-193.

Gholizadeh, M.H., Melesse, A.M., Reddi, L., 2016. A comprehensive review on water quality parameters estimation using remote sensing techniques. Sensors, 16(8), 1298.

Glembocki, N.G., Williams, G.N., Góngora, M.E., Gagliardini, D.A., Orensanz, J.M.L., 2015. Synoptic oceanography of San Jorge Gulf (Argentina): A template for Patagonian red shrimp (*Pleoticus muelleri*) spatial dynamics. Journal of Sea Research, 95, 22-35.

Gonzalez-Silvera, A., Santamaria-Del-Angel, E., Garcia, V.M.T., Garcia, C.A.E., Millán-Nuñez, R., Muller-Karger, F., 2004. Biogeographical regions of the tropical and subtropical Atlantic Ocean off South America: Classification based on pigment (CZCS) and chlorophyll-a (SeaWiFS) variability. Continental Shelf Research, 24, 983–1000.

Gordon, H.R., Brown, O.B., Evans, R.H., Brown, J.W., Smith, R.C., Baker, K.S., Clark, D.K., 1988. A semianalytic radiance model of ocean color. Journal of Geophysical Research: Atmospheres, 93(D9), 10909-10924.

Gregg, W.W., Conkright, M.E., Ginoux, P., O'Reilly, J.E., Casey, N.W., 2003. Ocean primary production and climate: global decadal changes. Geophysical Research Letters, 30(15).

Hernández-Moresino, R.D., Crespi-Abril, A.C., Soria, G., Sánchez, A., Isla, F., Barón, P.J., 2019. Inferring bottom circulation based on sediment pattern distribution in the San José Gulf, Patagonia Argentina. Journal of South American Earth Sciences, 89, 189-196.

Hernández-Moresino, R.D., Di Mauro, R., Crespi-Abril, A.C., Villanueva-Gomila, G.L., Compaire, J.C., Barón, P.J., 2017. Contrasting structural patterns of the mesozooplankton community result from the development of a frontal system in San José Gulf, Patagonia. Estuarine, Coastal and Shelf Science, 193, 1-11.

Hernández Moresino, R.D., Villanueva Gomila, L., Di Mauro, R., Barón, P.J., 2014. Structural differentiation of the mesozooplankton community in two hydrographic domains of a small basin: the frontal system of San José Gulf (Patagonia, Argentina) as a study case. Journal of plankton research, 36(2), 578-584.

Holligan, P.M., Williams, P.J.leB., Purdie, D., Harris, R.P., 1984. Photosynthesis, respiration and nitrogen supply of plankton populations in stratified, frontal and tidally mixed shelf waters. Marine Ecology Progress Series, 201-213.

Huot, Y., Babin, M., Bruyant, F., Grob, C., Twardowski, M.S., Claustre, H., 2007. Does chlorophyll a provide the best index of phytoplankton biomass for primary productivity studies? Biogeosciences discussions, 4(2), 707-745.

IOCCG (International Ocean-Colour Coordinating Group). 2000. Remote Sensing of Ocean Colour in Coastal and Other Optically-Complex Waters. S. Sathyendranath, ed., Reports of the International Ocean-Colour Coordinating Group, No. 3, IOCCG, Dartmouth, Canada, 140 pp.

Justić, D., Rabalais, N.N., Turner, R.E., Dortch, Q., 1995. Changes in nutrient structure of river-dominated coastal waters: stoichiometric nutrient balance and its consequences. Estuarine, Coastal and Shelf Science, 40(3), 339-356.

Kilham, P., Kilhamm S.S., 1980. The evolutionary ecology of phytoplankton. In: Morris, I. (Ed.), The physiological ecology of phytoplankton. University California Press, Berkley, pp 571–597.

Kratzer, S., Moore, G, 2018. Inherent optical properties of the baltic sea in comparison to other seas and oceans. Remote Sensing, 10, 418.

Krug, L.A., Platt, T., Sathyendranath, S., Barbosa, A.B., 2017. Unravelling region-specific environmental drivers of phytoplankton across a complex marine domain (off SW Iberia). Remote Sensing of Environment, 203, 162-184.

Krug, L.A., Platt, T., Sathyendranath, S., Barbosa, A.B., 2018. Patterns and drivers of phytoplankton phenology off SW Iberia: A phenoregion based perspective. Progress in Oceanography, 165, 233-256.

Lee, Z., Casey, B., Arnone, R.A., Weidemann, A.D., Parsons, R., Montes, M.J., …, Dye, J., 2007. Water and bottom properties of a coastal environment derived from Hyperion data measured from the EO-1 spacecraft platform. Journal of Applied Remote Sensing, 1(1), 011502.

Litchman, E., Klausmeier, C.A., 2008. Trait-based community ecology of phytoplankton. Annual review of ecology, evolution, and systematics, 39, 615-639.

Longhurst, A., 1998. Ecological geography of the sea. Academic Press, London, p. 398.

Lutz, V.A., Segura, V., Dogliotti, A.I., Gagliardini, D.A., Bianchi, A.A., Balestrini, C.F., 2010. Primary production in the Argentine Sea during spring estimated by field and satellite models. Journal of Plankton Research, 32(2), 181-195.

Lutz, V., Frouin, R., Negri, R., Silva, R., Pompeu, M., Rudorff, N., ..., Martinez, G., 2016. Bio-optical characteristics along the Straits of Magallanes. Continental Shelf Research, 119, 56-67.

Mann, K.H., Lazier, J.R.N., 2006. Dynamics of marine ecosystems: biological-physical interactions in the oceans. Blackwell Publishing, Malden, MA.

Margalef, R., 1978. Life-forms of phytoplankton as survival alternatives in an unstable environment. Oceanologica acta, 1(4), 493-509.

McQuatters-Gollop, A., Vermaat, J.E., 2011. Covariance among North Sea nutrient and climate drivers: consequences for plankton dynamics. Journal of Sea Research, 65(2), 284-292.

MODIS Mission page, 2019a. NASA Goddard Space Flight Center, Ocean Ecology Laboratory, Ocean Biology Processing Group. Moderate-resolution Imaging Spectroradiometer (MODIS) Aqua Inherent Optical Properties Data; 2018 Reprocessing. NASA OB.DAAC, Greenbelt, MD, USA. https://doi.org/ 10.5067/AQUA/MODIS/L3B/IOP/2018. Accessed on 07/08/2020

MODIS Mission page, 2019b. NASA Goddard Space Flight Center, Ocean Ecology Laboratory, Ocean Biology Processing Group. Moderate-resolution Imaging Spectroradiometer (MODIS) Aqua Chlorophyll Data; 2018 Reprocessing. NASA OB.DAAC, Greenbelt, MD, USA. https://doi.org/10.5067/AQUA/MODIS/L3B/CHL/2018. Accessed on 07/08/2020

MODIS Mission page, 2019c. NASA Goddard Space Flight Center, Ocean Ecology Laboratory, Ocean Biology Processing Group. Moderate-resolution Imaging Spectroradiometer (MODIS) Aqua Global Level 3 Mapped SST; 2019 Reprocessing. NASA OB.DAAC, Greenbelt, MD, USA. https://doi.org/10.5067/MODSA-MO4N9. Accessed on 07/08/2020

MODIS Mission page, 2019d. NASA Goddard Space Flight Center, Ocean Ecology Laboratory, Ocean Biology Processing Group. Moderate-resolution Imaging Spectroradiometer (MODIS) Aqua Photosynthetically Available Radiation Data; 2018 Reprocessing. NASA OB.DAAC, Greenbelt, MD, USA. https://doi.org/10.5067/ AQUA/MODIS/L3B/PAR/2018. Accessed on 07/08/2020

MODIS Mission page, 2019e. NASA Goddard Space Flight Center, Ocean Ecology Laboratory, Ocean Biology Processing Group. Moderate-resolution Imaging Spectroradiometer (MODIS) Aqua Euphotic Depth Data; 2018 Reprocessing. NASA OB.DAAC, Greenbelt, MD, USA. https://doi.org/10.5067/AQUA/MODIS/L3B/ ZLEE/2018. Accessed on 07/08/2020.

Morel, A., Prieur, L., 1977. Analysis of variations in ocean color 1. Limnology and Oceanography, 22(4), 709-722.

Orensanz, J.M., Parma, A.M., Ciocco, N., Cinti, A., 2007. Achievements and setbacks in the commercial diving fishery of San José Gulf, Argentine Patagonia. Fisheries management: Progress towards sustainability, 68-87.
Palma ED, Matano RP, Piola AR (2004) A numerical study of the Southwestern Atlantic shelf circulation: Barotropic response to tidal and wind forcing. J Geophys Res 109:C08014.

Palma, E.D., Matano, R.P., Piola, A.R., 2004. A numerical study of the Southwestern Atlantic Shelf circulation: Barotropic response to tidal and wind forcing. Journal of Geophysical Research: Oceans, 109(C8).

Papanikolopoulou, L.A., Smeti, E., Roelke, D.L., Dimitrakopoulos, P.G., Kokkoris, G.D., Danielidis, D.B., Spatharis, S., 2018. Interplay between r-and K-strategists leads to phytoplankton underyielding under pulsed resource supply. Oecologia, 186(3), 755-764.

Piola, A.R., Scasso, L.M., 1988. Circulación en el golfo San Matías. Geoacta, 15(1), 33-51.

Pisoni, J.P., Rivas, A.L., Piola, A.R., 2015. On the variability of tidal fronts on a macrotidal continental shelf, Northern Patagonia, Argentina. Deep Sea Research Part II: Topical Studies in Oceanography, 119, 61-68.

Richardson, A.J., Schoeman, D.S., 2004. Climate impact on plankton ecosystems in the Northeast Atlantic. Science 305, 1609–1612.

Rivas, A., Beier, E. (1990). Temperature and salinity fields in the Northpatagonic Gulfs. Oceanologica acta, 13(1), 15-20.

Rivas, A.L., Dogliotti, A.I., Gagliardini, D.A., 2006. Seasonal variability in satellite-measured surface chlorophyll in the Patagonian Shelf. Continental Shelf Research, 26(6), 703-720.

Rivas, A.L., Pisoni, J.P., 2010. Identification, characteristics and seasonal evolution of surface thermal fronts in the Argentinean Continental Shelf. Journal of Marine Systems, 79(1-2), 134-143.

Roelke D.L., Spatharis, S., 2015. Phytoplankton succession in recurrently fluctuating environments. PLoS One 10(3), e0121392.

Romero, S.I., Piola, A.R., Charo, M., Garcia, C.A.E., 2006. Chlorophyll-a variability off Patagonia based on SeaWiFS data. Journal of Geophysical Research: Oceans, 111(C5).

Sathyendranath, S., Watts, L., Devred, E., Platt, T., Caverhill, C., Maass, H., 2004. Discrimination of diatoms from other phytoplankton using ocean-colour data. Marine Ecology Progress Series, 272, 59–68.

Segura, V., Lutz, V.A., Dogliotti, A., Silva, R.I., Negri, R.M., Akselman, R., Benavides, H., 2013. Phytoplankton types and primary production in the Argentine Sea. Marine Ecology Progress Series, 491, 15-31.

Servicio de Hidrografía Naval (SHN), 1999. Carta Náutica H-214, De Faro Segunda Barranca a Faro Punta Bajos. Esc. 1: 275.000. Argentina.

Skalar Analytical® V.B, 2005a. Skalar Methods - Analysis: Nitrate + Nitrite - Catnr. 461-031 + DIAMOND Issue 081505/MH/99235956. Breda, The Netherlands.

Skalar Analytical® V.B, 2005b. Skalar Methods - Analysis: Phosphate - Catnr. 503-010w/r + DIAMOND Issue 081505/MH/99235956. Breda, The Netherlands.

Skalar Analytical® V.B, 2005c. Skalar Methods - Analysis: Silicate - Catnr. 565-051 + DIAMOND Issue 081505/MH/99235956. Breda, The Netherlands.

Smetacek, V., Cloern, J.E., 2008. On phytoplankton trends. Science, 319 (5868), 1346-1348.

Sommer, U., 1989. The role of competition for resources in phytoplankton ecology. In: Sommer, U. (Ed.), Plankton ecology: succession in plankton communities. Springer-Verlag, Berlin, pp. 57–106.

Strickland, J.D.H., Parsons, T.R., 1972. A practical handbook of seawater analysis. Fishery Research Board of Canada (second ed.), Bulletin 167, 310 pp.

Tonini, M.H., Palma, E.D., 2017. Tidal dynamics on the North Patagonian Argentinean gulfs. Estuarine, Coastal and Shelf Science, 189, 115-130.

Tonini, M., Palma, E., Rivas, A., 2006. Modelo de alta resolución de los Golfos Patagónicos. Mecánica Computacional, 1441-1460.

Venerus L. A.; A.M. Parma; D.E. Galván. 2008. Annual occupation pattern of temperate rocky reefs by the Argentine sandperch Pseudopercis semifasciata in San José Gulf Marine Park, Argentina. Fisheries Management and Ecology, 15, 217-229.

Wang, Y., Gao, Z., 2020. Contrasting chlorophyll-a seasonal patterns between nearshore and offshore waters in the Bohai and Yellow Seas, China: A new analysis using improved satellite data. Continental Shelf Research, 203, 104173.

Werdell, P.J., Franz, B.A., Bailey, S.W., Feldman, G. C., Boss, E., Brando, V. E., ..., Mangin, A.,2013. Generalized ocean color inversion model for retrieving marine inherent optical properties. Applied optics, 52(10), 2019-2037.

Werdell, P. J., McKinna, L. I. W., Boss, E., Ackleson, S. G., Craig, S. E., Gregg, W. W., Lee, Z., Maritorena, S., Roesler, C. S., Rousseaux, C. S., Stramski, D., Sullivan, J. M., Twardowski, M. S., Tzortziou, M., & Zhang, X. (2018). An overview of approaches and challenges for retrieving marine inherent optical properties from ocean color remote sensing. *Progress in Oceanography*, *160*(October 2017), 186–212. https://doi.org/10.1016/j.pocean.2018.01.001.

Williams, G. N., Dogliotti, A. I., Zaidman, P., Solis, M., Narvarte, M. A., González, R. C., Esteves, J. L., Gagliardini, D. A., 2013. Assessment of remotely-sensed sea-surface temperature and chlorophyll-a concentration in San Matías Gulf (Patagonia, Argentina). Continental Shelf Research, 52, 159-171.

Williams, G.N., Larouche, P., Dogliotti, A.I., Latorre, M.P., 2018b. Light absorption by phytoplankton, non-algal particles, and dissolved organic matter in San Jorge Gulf in summer. Oceanography, 31(4), 40-49.

Williams, G. N., Pisoni, J. P., Solís, M. E., Romero, M. A., Ocampo-Reinaldo, M., Svendsen, G. M., Curcio, N. S., Narvarte, M. A., Esteves, J. L., & González, R. A. C.,2021. Variability of phytoplankton biomass and environmental drivers in a semi-enclosed coastal ecosystem (San Matías Gulf, Patagonian Continental Shelf, Argentina) using ocean color remote sensing (MODIS) and oceanographic field data: Implications for fishery resources. *Journal of Marine Systems*, *224*(October 2020), 103615. https://doi.org/10.1016/j.jmarsys.2021.103615

Williams, G.N., Solís, M.E., Esteves, J.L., 2018a. Satellite-measured phytoplankton and environmental factors in North Patagonian Gulfs. In: Plankton Ecology of the Southwestern Atlantic. Springer, Cham, pp. 307-325.

Winder, M., Sommer, U., 2012. Phytoplankton response to a changing climate. Hydrobiologia, 698(1), 5-16.

Zhang, Y., Liu, X., Wang, M., Qin, B., 2013. Compositional differences of chromophoric dissolved organic matter derived from phytoplankton and macrophytes. Organic Geochemistry, 55, 26-37.

Highlights

A long-term bio-optical MODIS data in San José Gulf and adjacent waters were studied.

Additional spring and summer cruise data in the San José Gulf (SJG) was investigated.

Phytoplankton annual cycles respond to disparate nutrients/stratification/turbidity conditions.

East and west hydrographic domains in the SJG are evidenced for both data set.

Upwelling-downwelling structure in the east domain is driven by prevailing winds.

Conflict of Interest

The authors declare that they have no known competing financial interests or personal relationships that could have appeared to influence the work reported in this paper.